Vol. 36 (2005) *ACTA PHYSICA POLONICA B* No 12

S–P WAVE INTERFERENCE IN THE K^+K^- PHOTOPRODUCTION ON HYDROGEN*

Łukasz Bibrzycki, Leonard Leśniak

H. Niewodniczański Institute of Nuclear Physics, Polish Academy of Sciences
Radzikowskiego 152, 31-342 Kraków, Poland

Adam P. Szczepaniak

Physics Department and Nuclear Theory Center
Indiana University, Bloomington, IN 47405, USA

(Received September 26, 2005)

We have studied the partial wave interference effects to obtain a new information about the contribution of the S-wave to the cross section of the K^+K^- photoproduction on hydrogen. The K^+K^- photoproduction channel for the effective masses around 1 GeV is dominated by the $\phi(1020)$ resonance with only a small fraction of events coming from decays of scalar resonances $f_0(980)$ and $a_0(980)$. However, this S-wave admixture to the dominant P-wave leads to a measurable asymmetry in the angular distribution of outgoing kaons. A fairly precise estimation of the K^+K^- photoproduction cross section in the S-wave has been obtained.

PACS numbers: 13.60.Le, 25.20.Lj

1. Introduction

Both experimental and theoretical analyses of the near threshold photoproduction of the K^+K^- pairs are crucial for a better understanding of the nature of scalar mesons $f_0(980)$ and $a_0(980)$. Moreover, there exists a hypothesis that the $f_0(980)$ may be a $K\overline{K}$ bound state. The interest in the near threshold K^+K^- production dynamics and a relatively large coupling of the photon to vector mesons encouraged experimentalists to perform a series of experiments in seventies and eighties. Our investigations base on the results obtained by Behrend *et al.* [1] at DESY and Barber *et al.* [2] at the Daresbury Laboratory. These experiments showed unequivocally that the

* Presented at the XLV Cracow School of Theoretical Physics, Zakopane, Poland June 3–12, 2005.

S-wave participates in the K^+K^- photoproduction on hydrogen which can be seen in figures showing the moments of angular distribution as a function of the K^+K^- effective mass M_{KK}. However, in these early investigations the number of independent amplitudes taken into consideration was limited to three. This model limitation combined with large experimental uncertainties resulted in very big differences between the total cross sections reported by two experiments. The value of the total K^+K^- photoproduction cross section ranged from (2.7 ± 1.5) nb derived from the data of Behrend *et al.* to (96.2 ± 20) nb corresponding to the data of Barber *et al.* Contrary to previous experimental analyses we include all the independent amplitudes *i.e.* 4 amplitudes in the S-wave and 12 amplitudes in the P-wave. Moreover, our approach takes into account all 6 moments of angular distribution (including the moment $\langle Y_0^0 \rangle$ proportional to the effective mass distribution) which can be constructed from the spin 0 and spin 1 amplitudes. In the experimental analyses only two moments $\langle Y_0^0 \rangle$ and $\langle Y_0^1 \rangle$ were fitted. The data provided by two experiments correspond to two slightly different kinematic regions defined below:

1. $E_\gamma = 4$ GeV, $-t < 1.5$ GeV^2, 0.997 GeV$< M_{KK} <$1.042 GeV [2],
2. $E_\gamma = 5.65$ GeV, $-t < 0.2$ GeV^2, 1.005 GeV$< M_{KK} <$1.045 GeV [1].

Apart from analysing accessible data we have also applied the constructed model to the case of the incident photon energy $E_\gamma = 8$ GeV, corresponding to the value designed for the future energy upgraded facility at JLab [6].

2. Description of the model

Here we present very briefly only the most important ingredients of our model referring the reader to our previous papers [3–5] for a more extensive reading. The starting point of our investigation was the construction of the partial wave decomposed amplitudes for the K^+K^- photoproduction process. The amplitudes are defined by

$$T_{\lambda_\gamma\lambda\lambda'}(E_\gamma, t, M_{KK}, \Omega) = \sum_{L=0,1;M} T^L_{\lambda_\gamma\lambda\lambda';M}(E_\gamma, t, M_{KK}) Y^L_M(\Omega)\,, \quad (1)$$

where L and M denote the angular momentum of the K^+K^- subsystem and its projection on the helicity axis, λ_γ, λ and λ' are the helicities of the photon, the incoming proton and the outgoing proton, respectively, t is the momentum transfer squared and $\Omega = (\theta, \phi)$ denotes the solid angle of the outgoing K^+. The angles and momenta are defined in the so called s-channel helicity frame. This frame coincides with the K^+K^- rest frame in which the z-axis is directed opposite to the recoil proton momentum and the y-axis is perpendicular to the ϕp production plane.

2.1. S-wave amplitude

In our model the S-wave component of the K^+K^- photoproduction amplitude is parameterized by the t-channel exchange of the ρ and ω vector mesons. The amplitude has been decomposed into the isoscalar part and the isovector part in the following way:

$$A^S(I) = \frac{1}{2}\Big[A^S(I=0) + A^S(I=1)\Big]\,. \tag{2}$$

Additionally the amplitude has been factorized into the Born factor $A_j^B(I)$ and the factor $t_{jf}(I)$ responsible for the final state interactions according to the formula:

$$A^S(I) = \sum_{j=\pi\pi,K\overline{K}} A_j^B(I)\, t_{jf}(I)\,. \tag{3}$$

The Feynman graphs which contribute to the S-wave Born amplitudes are schematically shown in Fig. 1. The final state interaction factor $t_{jf}(I)$ is of the form $t_{jf}(I) \sim 1/2\,[\,\delta_{jf} + S_{jf}(I)\,]$. This factor accounts for the $\pi^+\pi^-$ and $\pi^0\pi^0$ intermediate states, and for the K^+K^- elastic rescattering.

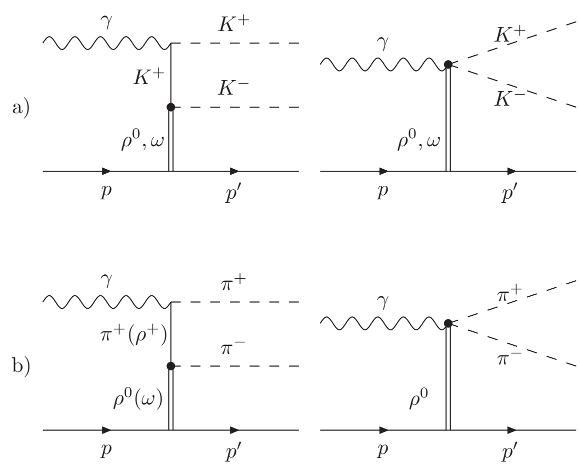

Fig. 1. Some diagrams representing the K^+K^- (a) and the $\pi^+\pi^-$ (b) Born photoproduction amplitudes.

The diagrams describing the S-wave amplitudes are schematically drawn in Fig. 2. The isoscalar S-matrix parameterized in terms of the channel phase shifts δ and inelasticity η reads:

$$S(I=0) = \begin{pmatrix} \eta e^{2i\delta_{\pi\pi}^{I=0}} & i\sqrt{1-\eta^2}e^{i(\delta_{\pi\pi}^{I=0}+\delta_{K\overline{K}}^{I=0})} \\ i\sqrt{1-\eta^2}e^{i(\delta_{\pi\pi}^{I=0}+\delta_{K\overline{K}}^{I=0})} & \eta e^{2i\delta_{K\overline{K}}^{I=0}} \end{pmatrix} . \quad (4)$$

The isovector S-matrix is defined analogously.

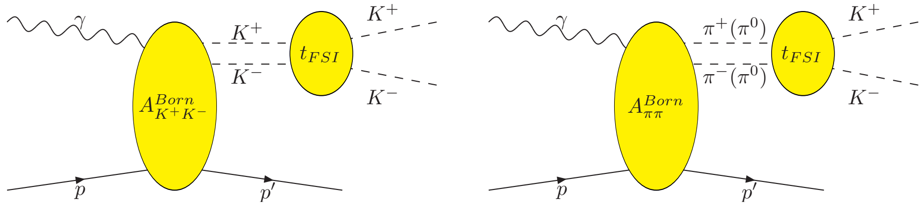

Fig. 2. Diagrams for elastic K^+K^- rescattering and inelastic $\pi\pi \to K^+K^-$ transition.

We use two kinds of propagators to describe the propagation of the ρ and ω mesons in the Born diagrams: the normal propagator $1/(t-m^2)$ or the Regge-type propagator

$$-\left[1-e^{-i\pi\alpha(t)}\right] \Gamma(1-\alpha(t)) \frac{(\alpha' s)^{\alpha(t)}}{(2s^{\alpha_0})} , \quad (5)$$

where m is the mass of the exchanged vector meson and $\alpha(t) = \alpha_0 + \alpha'(t-m^2)$ denotes the Regge trajectory of the vector meson in which $\alpha_0 = 1$ and $\alpha' = 0.9$ GeV^{-2}.

2.2. *P-wave amplitude*

We have assumed the pomeron exchange as a dominant reaction mechanism of the K^+K^- photoproduction in the P-wave. This approach is strongly supported by the OZI rule and previous experimental results. The Feynman diagram for the P-wave amplitude is shown in Fig. 3. The general form of the P-wave amplitude is

$$A^P_{\lambda_\gamma,\lambda,\lambda',M} = \overline{u}(p',\lambda') J^P_{\mu M} \varepsilon^\mu(q,\lambda_\gamma) u(p,\lambda) , \quad (6)$$

where q is the four-momentum of the incident photon, ε^μ is the polarization vector of the photon, p and p' are the four-momenta of the incoming and recoil proton, and the current $J^P_{\mu M}$ is defined as follows:

$$J^P_\mu = \frac{iF(t)}{M_\phi^2 - M_{KK}^2 - iM_\phi \Gamma_\phi} \left[\gamma^\nu q_\nu (k_1-k_2)_\mu - q^\nu (k_1-k_2)_\nu \gamma_\mu\right] . \quad (7)$$

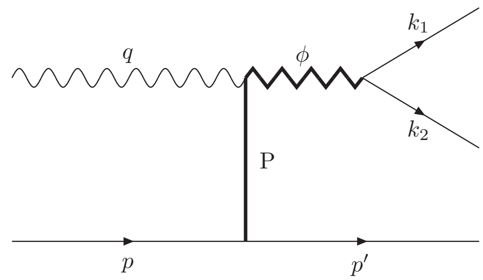

Fig. 3. Feynman diagram for the P-wave K^+K^- photoproduction on hydrogen.

The M_ϕ and Γ_ϕ denote the mass and width of the ϕ resonance, and k_1 and k_2 are the K^+ and K^- four-momenta. The function $F(t)$ is suitably parameterized to reproduce the experimental differential cross section $d\sigma/dt$ for the photon energies of 4 GeV or 5.65 GeV. Both the S- and P-wave amplitudes are Lorentz, gauge and parity invariant. For the sake of brevity we will denote the S-wave and P-wave amplitudes by S and P, respectively. To test our model and to make comparison with experimental data we have used the moments of angular distribution. Definitions of these moments read:

$$\begin{aligned}
\langle Y_0^0\rangle &= \frac{\mathcal{N}}{\sqrt{4\pi}}(|S|^2+|P_{-1}|^2+|P_0|^2+|P_1|^2)\,,\\
\langle Y_0^1\rangle &= \frac{\mathcal{N}}{\sqrt{4\pi}}(SP_0^*+S^*P_0)\,,\\
\langle Y_1^1\rangle &= \frac{\mathcal{N}}{\sqrt{4\pi}}(P_1S^*-SP_{-1}^*)\,,\\
\langle Y_0^2\rangle &= \frac{\mathcal{N}}{\sqrt{4\pi}}\sqrt{\frac{1}{5}}(2|P_0|^2-|P_1|^2-|P_{-1}|^2)\,,\\
\langle Y_1^2\rangle &= \frac{\mathcal{N}}{\sqrt{4\pi}}\sqrt{\frac{3}{5}}(P_1P_0^*-P_0P_{-1}^*)\,,\\
\langle Y_2^2\rangle &= \frac{\mathcal{N}}{\sqrt{4\pi}}\sqrt{\frac{6}{5}}(-P_1P_{-1}^*)\,, \qquad (8)
\end{aligned}$$

where $\mathcal{N}$ is the normalization factor. In formulas (8) the summation over the photon and proton helicities is implicit.

3. Numerical calculations

We have introduced the complex parameters multiplying the S-wave and P_0 amplitudes to account for some phenomenological effects. The background present in the K^+K^- mass distribution and moments was param-

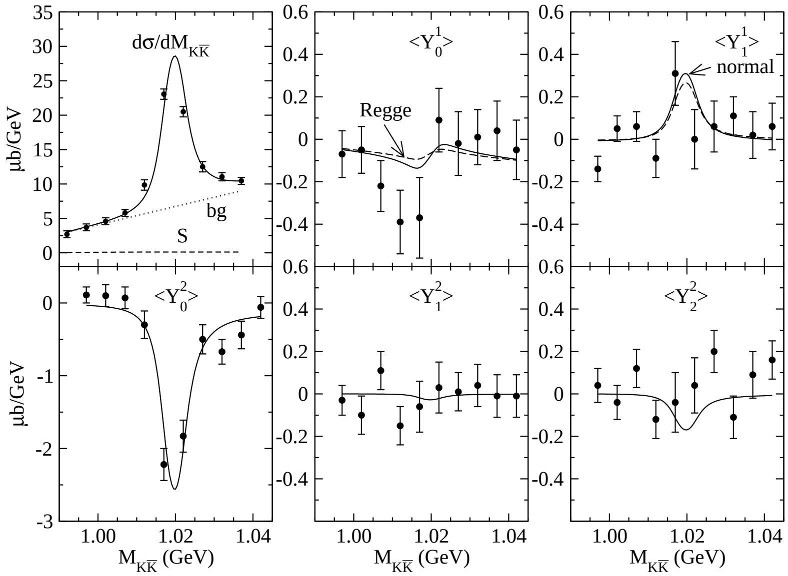

Fig. 4. Effective mass distribution and moments at $E_\gamma = 4$ GeV. The experimental data are from [2]. The curves marked by S and bg denote the S-wave cross section and the background, respectively.

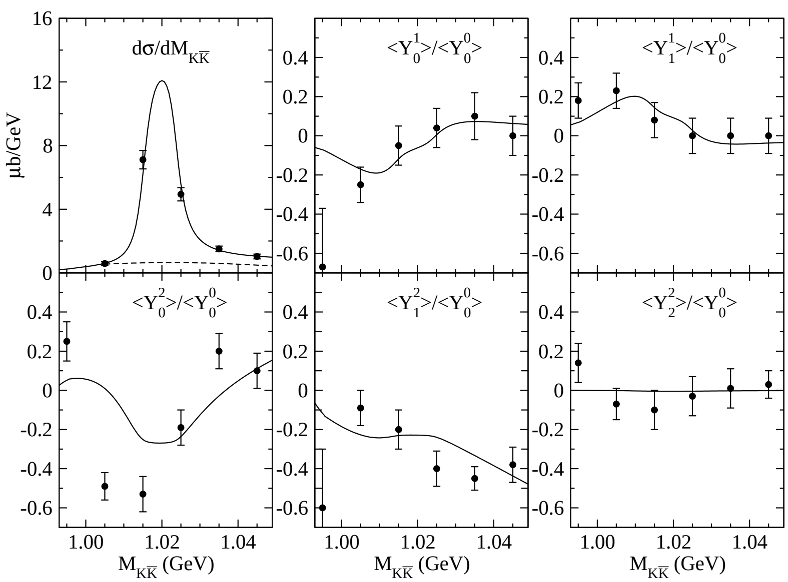

Fig. 5. Effective mass distribution and moments at $E_\gamma = 5.65$ GeV. The experimental data are from [1].

eterized using linear functions of M_{KK} thus adding new parameters. The total number of the model parameters to be fitted was 9 for the Daresbury data and 8 for the DESY data. Results of our numerical calculations for the incident photon energies of 4 GeV and 5.65 GeV are shown in Figs. 4 and 5, respectively.

In these figures one can see a very good agreement of the model with experimental data. The values of cross sections, expressed in nanobarns and computed using phenomenological parameters obtained in the minimization procedure, are shown in Table I.

TABLE I

Integrated cross sections in nanobarns.

Photon energy	4 GeV		5.65 GeV	
S-wave propagator	normal	Regge	normal	Regge
Sum of P-waves	218.4 ± 39.5		120.5 ± 9.4	
P_0-wave	$6.4^{+5.5}_{-4.8}$	$4.7^{+5.7}_{-4.5}$	$13.8^{+5.3}_{-4.7}$	$14.0^{+5.3}_{-4.8}$
S-wave	$4.9^{+5.8}_{-3.6}$	$4.3^{+6.6}_{-3.6}$	$7.0^{+6.8}_{-4.4}$	$6.8^{+6.6}_{-4.3}$
background	$299.4^{+10.0}_{-10.4}$	$300.0^{+10.0}_{-10.7}$	$4.5^{+4.3}_{-6.1}$	$4.7^{+4.2}_{-5.8}$
$\lvert t\rvert_{\max}$	1.5 GeV^2		0.2 GeV^2	
M_{KK} range	(0.997,1.042) GeV		(1.01,1.03) GeV	

The most interesting result of this calculation is the value of S-wave total cross section. Using the normal propagators its value varies from 4.9 to 7 nb for two analyzed photon energies. For the Regge propagators the values are quite similar. This strongly supports the estimation of the S-wave photoproduction cross section made by the DESY group of Behrend *et al.*

We have also applied the model constructed to compute the mass distribution and the moments of the angular distribution for the incident photon energy of $E_\gamma = 8$ GeV which is the energy designed for the upgraded JLab accelerator facility [6]. Results of these calculations are shown in Fig. 6.

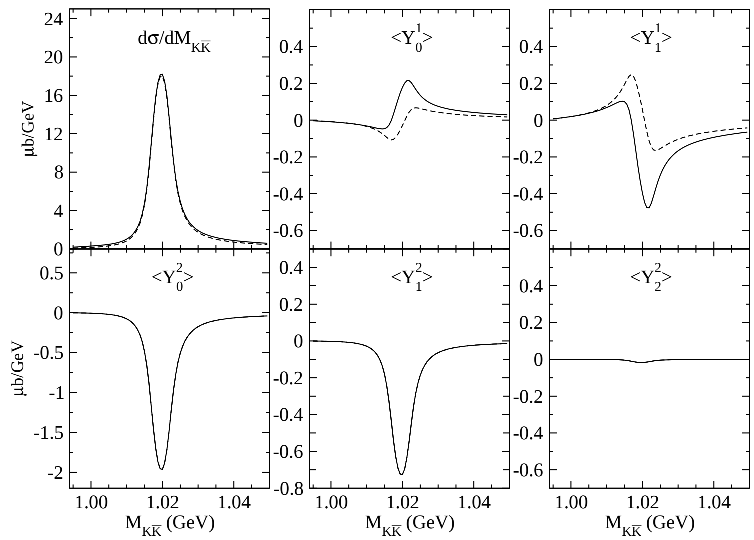

Fig. 6. Prediction for the mass distribution and moments at $E_\gamma = 8$ GeV.

4. Summary and outlook

We have shown that the S-wave contribution to the elastic K^+K^- photoproduction gives a measurable effect. Our model supports the lower estimation of the S-wave total photoproduction cross section with the values between 4.9 and 7 nb. The natural consequence of these studies is an examination of the other production reactions where partial wave interference may take place. The $\pi^+\pi^-$ photoproduction (or electroproduction) on hydrogen is an obvious choice. One may expect an appearance of the interference effects from the ρ-dominated P-wave and from the $f_0(980)$ resonance in the S-wave. The recent results obtained by the HERMES collaboration [7] which indicate a possible contribution from the $f_0(980)$ resonance in the S-wave and $f_2(1270)$ in the D-wave make this investigation even more interesting.

REFERENCES

[1] H.-J. Behrend *et al., Nucl. Phys.* **B144**, 22 (1978).
[2] D.P. Barber *et al., Z. Phys.* **C12**, 1 (1982).
[3] C.-R. Ji, R. Kamiński, L. Leśniak, A.P. Szczepaniak, R. Williams, *Phys. Rev.* **C58**, 1205 (1998).
[4] L. Leśniak, A.P. Szczepaniak, *Acta. Phys. Pol. B* **34**, 3389 (2003).
[5] Ł. Bibrzycki, L. Leśniak, A.P. Szczepaniak, *Eur. Phys. J.* **C34**, 335 (2004).
[6] A.R. Dzierba, *Int. J. Mod. Phys.* **A18**, 397 (2003).
[7] A. Airapetian *et al., Phys. Lett.* **B599**, 212 (2004).